Impact of past steel-making activities on lanthanides and Y (REY) fractionation and potential mobility in riverbank sediments

Christophe Hissler, Emmanuelle Montargès-Pelletier, Hussein Kanbar, Mathieu Le Meur, Christophe Gauthier

Impact of past steel-making activities on lanthanides and Y (REY) fractionation and potential mobility in riverbank sediments

Christophe Hissler[1*], Emmanuelle Montarges-Pelletier[2], Hussein J. Kanbar[2], Mathieu Le Meur[2], Christophe Gauthier[2]

[1]Luxembourg Institute of Science and Technology (LIST), Luxembourg, [2]UMR7360 Laboratoire Interdisciplinaire des Environnements Continentaux (LIEC), France

Submitted to Journal:
Frontiers in Earth Science

Specialty Section:
Geochemistry

Article type:
Original Research Article

Manuscript ID:
1056919

Received on:
29 Sep 2022

Revised on:
17 Dec 2022

Journal website link:
www.frontiersin.org

Conflict of interest statement

The authors declare that the research was conducted in the absence of any commercial or financial relationships that could be construed as a potential conflict of interest

Author contribution statement

CH and EMP contributed to the conceptualization, the data curation and treatment, the designing, writing and final editing of the manuscript, the supervision and administration of the project. HJK, ML and CG participated in the draft manuscript review and final editing. EMP, HJK, ML and CG performed the core sediment sampling, the bulk sample preparation and analysis. CH performed the sequential extractions.

Keywords

Rare earth element, pollution, River sediment, Mineralogy, industrial valley

Abstract

Word count: 299

New technologies significantly disturb the natural riverine cycle of some Rare Earth Elements and Yttrium (REY). Whereas large evidence exists on the anthropogenic impact on REY dissolved and colloidal loads in rivers, there is still a knowledge gap on how suspended load could be impacted. As the river suspended matter is a key driver for the quantity of trace metal transport and mobility toward the other river compartments, it is of importance to evaluate how anthropogenic activity could affect its REY composition. Here, we report how past steel-making processes impacted the REY composition and potential mobility in riverbank sediments collected from a French River basin heavily disturbed by this industrial activity. In comparison to sediment originated from the local soil erosion, the industrial waste released in the river presented very unusual REY patterns. We observed specific LaN/GdN, LaN/LuN and Y/Ho ratios that indicate a strong heritage in the industrial waste of the iron ore used to produce steel. REY enrichments were also highlighted and can be classified as follow: Eu>Yb>Sm>Ce>Tm. The different enrichments might illustrate various fractionation processes that occurred separately on the different lanthanides inside the blast furnace according to temperature, pressure and oxygen fugacity changes. Sequential extractions performed on natural and industrial waste samples showed that REY enrichments in the industrial waste are included in one main fraction, which is strongly labile, whereas REYs contained in the sediment originating from the soil erosion are related to different mineralogical fractions having lower and more specific lability. Finally, REY composition showed that the sediment deposited on the riverbank is composed of two types of materials, which progressively evolved, after the ending of the industrial activity in this region, from a pure industrial waste in depth to a pure natural suspended sediment originated from local soil erosion at the surface.

Contribution to the field

The present study investigates REY distribution and origins in three riverbank cores of a heavily polluted river system, Northeastern France; two of those banks were proven to be full made of steel-making wastes. We examined the evolution of the REY patterns in those materials as a function of depth and hypothesize that steel-making waste presented a contrasting REY pattern due to the temperature and redox conditions inside the blast furnace during ore melting, such conditions were able to enhance fractionation between lanthanides. We also demonstrate that REY present in the blast furnace sludge might have a different mobility potential in comparison to the detrital suspended particles, originated from soil erosion. These findings may be used to assess more precisely the impact of anthropogenic activities in river systems by using REY as tracer of pollution dissemination in such aquatic ecosystems.

Funding statement

This research was funded by the Luxembourg National Research Fund (FNR) and the French National Research Agency (ANR-14-CE01-0019) in the framework of the FNR INTER ANR research program (contract no. INTER/ANR/13/9441502). The Long-Term Ecosystem Research (LTER) France, the French Water Agency Rhin-Meuse and the Region Lorraine through the research network of the Zone Atelier Moselle (ZAM) partially funded this work.

Ethics statements

Studies involving animal subjects
Generated Statement: No animal studies are presented in this manuscript.

Studies involving human subjects
Generated Statement: No human studies are presented in this manuscript.

Inclusion of identifiable human data
Generated Statement: No potentially identifiable human images or data is presented in this study.

Data availability statement

Generated Statement: The datasets presented in this study can be found in online repositories. The names of the repository/repositories and accession number(s) can be found below: https://doi.org/10.24396/ORDAR-59 and https://doi.org/10.5281/zenodo.7447548.

Impact of past steel-making activities on lanthanides and Y (REY) fractionation and potential mobility in riverbank sediments

Christophe Hissler[1*], Emmanuelle Montarges-Pelletier[2,3], Hussein J. Kanbar[2,3], Mathieu Le Meur[2,3], Christophe Gauthier[2,3]

[1] CAT/ENVISION/ERIN Research Group, Luxembourg Institute of Science and Technology, L-4422 Belvaux, Luxembourg

[2]LIEC, CNRS, Université de Lorraine, F-54000 Nancy, France

[3]LTSER FRANCE Zone atelier Moselle

***Correspondence:**
Christophe Hissler
christophe.hissler@list.lu

Keywords: rare earth elements, pollution, river sediment, mineralogy, industrial valley

Abstract

New technologies significantly disturb the natural riverine cycle of some Rare Earth Elements and Yttrium (REY). Whereas large evidence exists on the anthropogenic impact on REY dissolved and colloidal loads in rivers, there is still a knowledge gap on how suspended load could be impacted. As the river suspended matter is a key driver for the quantity of trace metal transport and mobility toward the other river compartments, it is of importance to evaluate how anthropogenic activity could affect its REY composition. Here, we report how past steel-making processes impacted the REY composition and potential mobility in riverbank sediments collected from a French River basin heavily disturbed by this industrial activity. In comparison to sediment originated from the local soil erosion, the industrial waste released in the river presented very unusual REY patterns. We observed specific La_N/Gd_N, La_N/Lu_N and Y/Ho ratios that indicate a strong heritage in the industrial waste of the iron ore used to produce steel. REY enrichments were also highlighted and can be classified as follow: Eu>Yb>Sm>Ce>Tm. The different enrichments might illustrate various fractionation processes that occurred separately on the different lanthanides inside the blast furnace according to temperature, pressure and oxygen fugacity changes. Sequential extractions performed on natural and industrial waste samples showed that REY enrichments in the industrial waste are included in one main fraction, which is strongly labile, whereas REYs contained in the sediment originating from the soil erosion are related to different mineralogical fractions having lower and more specific lability. Finally, REY composition showed that the sediment deposited on the riverbank is composed of two types of materials, which progressively evolved, after the ending of the industrial activity in this region, from a pure industrial waste in depth to a pure natural suspended sediment originated from local soil erosion at the surface.

1 Introduction

Since the end of the 18th century and the technical process to eliminate the phosphorus contained in the iron ore (Garcier, 2007), northern-western European countries, including the Lorraine region in France, have been more active with iron and coal mining and related steel production. To ensure an

easy access to water source to the production facility, unforeseen changes were brought to the river ecosystems, profoundly modifying the riparian landscape by physical, chemical and biological changes (Picon, 2014). River water served in several steel-making processes, such as a cleaning fluid for an efficient use of the blast furnace and as the receptacle of industrial wastes. Industrial wastes of many different origin and composition (furnace smokes, dust and sludge from wet cleaning of furnace smokes) were since then directly introduced in the river channel, transported as suspended particles or stored in the riverbed (Vdović et al., 2006; Zebracki, 2008; Kanbar et al., 2017).

All these changes in the riverbed disturbed the natural cycle of elements, and in particular that of critical elements used for the technology development. Bau and Dulski (1996) published for the first time scientific evidence of an anthropogenic impact on the REY natural cycle. Since then, REY are studied as emergent micropollutants because of their widespread use in industrial and medical activities (Zhang et al., 2017; Knobloch et al., 2018). The various anthropogenic uses are associated with so-called REY anomalies in fluvial systems worldwide (Kulaksiz and Bau, 2013). The most famous is the positive Gd anomaly, related to the clinical use of Gd-based contrast agents in Magnetic Resonance Imaging (MRI), which is now considered worldwide as a distinctive signature of water inputs from wastewater treatment plants (Merschel et al., 2015; Parant et al., 2018; Louis et al., 2020). Until now, Gd-based contrast agents are recognized as unreactive in the environment and the corresponding Gd anomaly occurs only in the truly dissolved fraction, defined as the fraction passing through 10 kDa ultrafiltration membranes. In most recent studies, river colloidal fractions (10 kDa – 1000 nm) were also subject of REY contamination due to the effluents of a production plant for fluid catalytic cracking catalysts using La and Sm (Kulaksiz and Bau, 2013; Klaver et al., 2014) or to steel making activity for Nd (Martin et al., 2021). It is generally admitted that most of the REY transported by suspended particle matter, (particles >1000 nm) present a natural signature like soils and bedrocks in little river systems (Hissler et al., 2016). Such signature was also highlighted for larger rivers such as the Congo, Amazon, Mississippi, Ohio, and Rhine rivers (Goldstein and Jacobsen, 1988; Eldefield et al., 1990; Dupré, 1996; Tricca et al., 1999). Despite the discovery of anthropogenic REY in dissolved and colloidal fractions of river water, only few studies observed anthropogenic impact on the REY contents of river suspended particulate matter. La anomaly was observed by Klaver et al. (2014) in the Rhine River basin. Hissler et al. (2015a and 2016) and Martin et al. (2021) identified a positive Ce and Nd anomalies in river suspended particulate matter linked to current and historical Luxembourg steel-making activities in the upper Alzette River basin. All these results strengthen how the increasing extraction and use of REY is disrupting their natural biogeochemical cycles in polluted rivers. The harmful effects of REY are not solely linked to the relatively recent production of technology tools, but also to historical anthropogenic activities, as well as those involving steel-making. To date, the environmental risk of REY has received little attention because it is perceived as relatively low in comparison to other more abundant metals. Moreover, the forms in which anthropogenic REY are stored in river sediments and the processes that control their mobility from sediment to the water column need to be further investigated to evaluate potential biological and human health threats (Lachaux et al., 2022).

The present study investigates REY distribution and origins in three riverbank cores of the Orne River, Northeastern France; two of those banks were proven to be full made of steel-making wastes, such as blast furnace sludge (Kanbar et al., 2017; Kanbar, 2017). We examined the evolution of the REY patterns in those materials as a function of depth and hypothesize that steel-making waste presented a contrasting REY pattern due to the temperature and redox conditions inside the blast furnace during ore melting, such conditions were able to enhance fractionation between lanthanides. We also demonstrate that REY present in the blast furnace sludge might have a different mobility potential in comparison to the detrital suspended particles, originated from soil erosion. These findings may be

used to assess more precisely the impact of anthropogenic activities in river systems by using REY as tracer of pollution dissemination in such aquatic ecosystems.

2. Material and methods

2.1. Study site

From 1880 to 2008, the Lorraine region (North-East of France) had an industrial and economical importance for the steel production in France and Europe. In this context, due to the local occurrence of iron ore, the Orne River basin was subject to intense steel-making activity, including iron mining, coke, pig iron and steel production. This industrialization severely modified the physics and chemistry of the Orne River and its major riverbed. The reminiscent impact of this past industry on the Orne River geomorphology, banks and water quality were also already referenced in several studies (Abuhelou, 2016; Kanbar et al, 2017; Losson et al., 2020; Martinez-Carreras et al., 2021). In the beginning of the steel-making industry and during almost the whole period of this activity, tons of blast furnace sludge and other fine particle suspensions were daily discharged in the Orne River, provoking lateral floods due to the filling of the main river course. The amount of suspended particles introduced in the river was estimated to be 31t per day in 1972. Dredging was lately operated in the 60's and 80's, leaving contaminated banks for several kilometers. In the last period of the steel-making activity, to guarantee sufficient water resource for the cooling of furnaces, two dams were built (1960 for Moyeuvre Grande dam and 1973 for Homecourt dam). Those dams, following the European water rules, were recently opened, showing up the banks made of industrial wastes.

The Orne River joins the Moselle River and belongs to the Rhine River basin. This river flows in the northeastern France, is 90 km long from its source in Ornes to the confluence with the Moselle River in Richemont and has a basin area of 1,268 km^2 (Fig. 1). The geology of the Orne River basin can be divided into two main parts, (i) a clayey depression in the Woëvre region made of easily eroded soft Lias marl lithologies and (ii) a calcareous plateau at the Pays-Haut, starting in Jarny and belonging to middle Jurassic lithologies, an Aalenian calcareous sandstone and some Bajocian limestones. The Aalenian calcareous sandstone is a ferriferous formation used as iron ore in this region. It is made of an oolitic ferriarenite that includes more than 10 layers, each layer being several meters thick.

Figure 1: The Orne River basin, the downstream area where steel-making facilities and dams were installed and a focus on the influence zone (orange dashed line) of the Moyeuvre dam, also called Beth dam with the location and the log description of the three riverbank cores selected in this study (from upstream to downstream: JOSAN, JOEP and BETHUP).

2.2. Sampling and sample preparation

The cores were sampled at three distinct places, all located in the influence zone of the Beth dam (figure 1). This dam was operating from 1960 to 2019 providing a water reservoir for blast furnace cooling between 1960 and 1980. The most upstream site, JOSAN, is located in the beginning of the influence zone, on the right side of the river. The bank was cored in 2015 using a 9 cm tube diameter from a floating platform (Quadriraft from GEHCO laboratories, Tours University, France). The core was 51.5 cm long. The second core site, JOEP is located in the very end of the first division of Jœuf steel-making site. This zone was dredged in 1988, the riverbanks are not natural, and the flowing waters incised the riverbed. The bank was cored in 2017 using a piston corer (diameter 6 cm). The core was 82 cm long. The last core (BETHUP) was sampled downstream on the right bank few dozen meters before the Beth

dam (Kanbar et al 2017) in 2014. The core was 131 cm long. The location and characteristics of the three cores are provided in Figure 1.

After coring, the tubes were filled with flower foam to minimize the air volumes and were hermetically closed with plastic caps and thick tape. Back to the laboratory, the cores were cut lengthwise, and one half was immediately stored in a glove bag with N_2 gas flow to prevent oxidation. After deep examination of the core physical aspects, texture and color, 2 to 3 cm slices were cut. The different slices were weighed, frozen at -18 °C and freeze-dried. The final amount of freeze-dried sediments was weighed and water content was calculated. For each slice, 1.5 g aliquot was sampled after soft homogeneization, and was ground. The ground samples were used for element analysis.

A sequential leaching extraction was performed on aliquots of two freeze-dried samples from JOSAN and JOEP cores; they represent the recent deposition at the surface of the riverbed and the historical steel waste that can be found at the bottom of the core sediments, respectively. The used procedure (Hissler et al., 2015b), adapted from Steinmann and Stille (1997), allows to identify the mobile and labile part of the sediment and to recover the leachable fractions, which are considered to represent adsorbed elements and those fixed in acid-soluble phases. With this technique, we assume that the residual fraction and the different leachable fractions are operationally defined because of the existing continuum between residual and leachable phases (Stille and Clauer, 1994). Sequential leaching was performed in four steps using demineralized MilliQ water (Millipore system – L1 leachate), acetic acid (0.05N Hac – L2 leachate), hydrochloric acid (1N HCl – L3 leachate) and nitric acid (2N HNO_3 – L4 leachate). All these reagents are of ultrapure quality and the measured blanks were always below the detection limit.

2.3. REY and related major element analysis

Major (Na, Mg, K, Ca, Al, Mn, Fe, Si and P) and REY (La, Ce, Pr, Nd, Sm Eu, Gd, Tb, Dy, Ho, Er, Tm, Yb, Lu and Y) were detected in the bulk sediments, the bedrocks and in the leaching residual sediment fractions by inductively coupled plasma optical emission spectrometry (ICP-OES) and inductively coupled plasma mass spectrometry (ICP-MS), respectively. These analyses were performed at SARM (Service d'Analyse des Roches et des Minéraux – CRPG, Vandoeuvre-lès-Nancy, France) and all analytical methods were subject to QC/QA procedures using certified reference materials (Carignan et al., 2001). The associated results can be found on the ORDAR data repository (https://doi.org/10.24396/ORDAR-59).

The major and trace elements concentrations of the leachates were determined using ICP-MS (Agilent 7900) associated with an ISIS 3 (Agilent) injection system at LIST. Analyses were conducted in He mode and ^{103}Rh and ^{185}Re were used as internal standards. Analytical blank values were less than 1% of the lowest sample concentrations for all elements. For all REY, the detection limit was 0.3 ng L^{-1} and the quantification limit was 1.0 ng L^{-1}. Calibration standards were prepared with Multi elements ICP standard solutions (CHEM-LAB Analytical) diluted in 1% HNO_3. We calculated the mass balance during the complete sequential extraction for each analyzed element and we compared the total concentrations obtained by sequential extraction (L1+L2+L3+L4+residu) to that obtained on the bulk sample. For a given element, the two total concentrations presented differences but were significantly correlated for both major and REY elements with R^2 of 0.99 for JOSAN and JOEP, illustrating that the differences are consistent between most of the elements for the two samples, only Ca presented more contrasted results. JOSAN had close total concentrations between the two methods, whereas sequential extraction on JOEP showed higher total concentrations for most of the elements. This could be attributed to heterogeneities in the two JOEP aliquots used for both methods. The associated results can be found on a Zenodo data repository (https://doi.org/10.5281/zenodo.7447548).

2.4. Mineralogy

X-ray diffraction (XRD) analyses were performed at LIEC laboratory on the bulk ground sediment layers to determine the major crystalline phases. A D8 Advance Bruker diffractometer with a Co $K_{\alpha 1}$ radiation source, operated at 35 kV and 45 mA (λ = 1.7902 Å), was used. XRD patterns were collected on the angular range (2θ) of 3 – 64°, with a 0.034° step size and a 3 sec collecting time. All layers were subjected to XRD analyses, and for clearness purpose, only relevant patterns are presented.

2.5. REY anomaly calculations

The unusual REY patterns that were observed in the studied samples make the quantification of the relative REY anomalies difficult. For this reason, we assumed that some REY elements are not impacted during the described processes and can be used as reference element to calculate anomalies for the impacted elements during the melting process of the steel production. This important issue is also discussed more in detail in §4.2.

The calculation of the REY anomalies are given below:

$$Ce/Ce^* = Ce/(\tfrac{1}{2}La + \tfrac{1}{2}Pr) \quad \text{eq. 1}$$

$$Sm/Sm^* = Sm/(\tfrac{2}{3}Nd + \tfrac{1}{3}Gd) \quad \text{eq. 2}$$

$$Tm/Tm^* = Tm/(\tfrac{2}{3}Er + \tfrac{1}{3}Lu) \quad \text{eq. 3}$$

$$Yb/Yb^* = Yb/(\tfrac{1}{3}Er + \tfrac{2}{3}Lu) \quad \text{eq. 4}$$

3. Results

3.1. mineralogy, major element contents and distributions along the core profiles

JOSAN sediments display a detrital X-ray diffraction pattern, predominated by clay minerals, quartz and feldspars as silicates, and by calcite as carbonates (Fig. 2a). JOSAN core was described as a series of silt, clay layers and leaf layers (Kanbar, 2017; De la Cruz Barrón et al., 2018). The clay minerals are mainly constituted of illite, interlayered illite/smectite and chlorite. In a previous publication (De la Cruz Barrón et al., 2018), we could evidence the similarity between clay mineralogy of the Orne River suspended particulate matter and the surface sediments sampled in JOSAN. With depth, the mineralogy of JOSAN does not show strong modifications, the apparent amount of quartz and calcite follows the particle size distribution and the organic matter content.

The mineralogy of BETHUP core was previously described (Kanbar et al., 2017). Below surface sediments that display a detrital mineralogical fingerprint like that of JOSAN samples (quartz, calcite, feldspars, and clay minerals), steel-making wastes can already be observed. This is proven by iron bearing phases, oxides and (hydr)oxides, ferrous and ferric, crystalline and non-crystalline phases. The iron phases are assigned to dust particles from the blast furnaces (wustite FeO, magnetite Fe_3O_4), to pristine iron ore (goethite FeOOH) and to weathering products (Fe-clays). The relatively low intensity of quartz diffraction lines and the presence of iron oxide diffraction lines in the 38-45 2Θ region are the main characteristics of the XRD patterns of those steel-making wastes (Fig. 2a, curves 4 and 5). JOEP material displays similar mineralogy to BETHUP deposit with a relatively lower content of iron

crystalline phases (wustite, magnetite), but displaying goethite, the main iron phase of the iron ore (Dagallier et al., 2002, Kanbar et al., 2017). Goethite particles in BETHUP and JOEP materials are shown to be similar in shape, crystallinity and composition to the goethite of iron ore, which is the Aalenian calcareous sandstone (Kanbar et al., 2017). JOEP material appears relatively enriched in calcite (Fig. 2b). The origin of such high amount of calcium carbonates was assumed to be related to the regular inputs of lime in the river (Garcier et al 2007), also evidenced by thin white layers (Fig. 2c). Beside industrial borne minerals, JOEP and BETHUP cores still display a low contribution of detrital materials (Fig. 2a, curves 4 and 5).

Figure 2: a. XRD patterns for JOSAN, JOEP and BETHUP samples. The three top curves correspond to surface sediments at the three river stations from upstream to downstream: 1: JOSAN surface sediment; 2: JOEP surface sediment; 3: BETHUP surface sediment. The two bottom curves represent deep layers of JOEP (4) and BETHUP (5) cores. Abbreviations of mineral phases: quartz (Q); calcite (C); Feldspars (F); clay minerals (CM); magnetite (M); goethite (G); wustite (W); Fe-clays (FeC).

b. zoom on calcite diffraction lines for deep samples at JOEP (4) and BETHUP (5).

c. observation of the thin white calcium layers at JOEP

The evolution of the major element contents in the bulk BETHUP samples show three groups (Fig. 3a). Si, Na, Al, K and Ti contents progressively decrease with depth and present strong linear correlations (Kanbar et al., 2017). On the contrary, elements of the second group, Fe, Mn and P have a content progressively increasing with depth and present strong linear anti-correlations with Si and other alkaline elements. The last group corresponds to Mg and Ca contents that do not present any significant evolution trend with depth. Ca profile is partly related to the input of lime sludge in the river during the industrial activity. A very similar vertical evolution with depth is also observed for the core collected at JOEP and similar groups can be defined (Fig. 3b). The major element contents measured in the core collected at JOSAN present different results (Fig. 3c). Si and Fe are close to the values found in the Group I, whereas Ca is higher and increases with depth.

3.2. REY patterns and content in the local lithologies and the bulk core layers

REY contents are in the same order of magnitude for the three main lithologies that cover the studied river basin (Fig. 4a). By normalizing to the Post-Archean Australian Shale (PAAS, Taylor and McLennan, 1985), they show very distinct types of distribution patterns (Fig. 4a). While the Toarcian marls have a flat pattern with a slight middle REY (from Sm to Tb) enrichment, shown by Eu/Eu^* anomaly of 1.2, the Bajocian limestone present a strong Ce negative anomaly ($Ce/Ce^*=0.5$) and is depleted in heavy REY (from Dy to Lu) with $La_N/Lu_N=2.1$. Both lithologies display larger Y/Ho ratios of 32 and 105, respectively. The Aalenian calcareous sandstone, which includes the iron ore used for the steel production in this area, has a PAAS-normalized REY pattern characterized by a large depletion in light REY (from La to Nd), with $La_N/Lu_N=0.4$, and a lower Y/Ho ratio of 24.

The REY contents of surface sediments lie in the same range as those of the lithologies. However, a decrease can be observed down the cores for JOEP and BETHUP. From the surface to the bottom of the BETHUP (Fig. 4b) and JOEP (Fig. 4c) cores, the REY patterns can be separated in four groups according to the Si and Fe contents (Kanbar et al., 2017). At JOSAN, only two different groups can be distinguished (Fig. 4d). The calculated PAAS-normalized patterns evolve coherently between the groups with the SiO_2 content at the three locations. Close to the surface, the patterns are flat (average

La_N/Lu_N=1.0) with a little middle REY enrichment (average Eu/Eu^*=1.1) (Fig. 4bcd). In the bottom layers of the BETHUP and JOEP cores, the PAAS-normalized REY patterns look very unusual according to what is known in Earth Critical Zone environments (Fig. 4bc). The main characteristics of these patterns are a light REY depletion (average La_N/Lu_N=0.5) and multiple enrichments in several lanthanides that can be characterized by the related anomalies: Ce/Ce^* (1.1), Sm/Sm^* (1.5), Eu/Eu^* (1.7), Tm/Tm^* (1.2) and Yb/Yb^* (1.4) (Fig. 4bc). The REY pattern of the samples located between the surface and the deepest layer present a coherent and regular evolution with depth in between these two samples, as illustrated by the Y/Ho ratio evolution with depth at BETHUP (Fig. 3a).

Figure 3: Evolution with depth of Si, Fe and Ca contents, as atomic percentage, and the REY pattern characteristics observed in the core collected from the Orne Riverbank at (a) BETHUP, (b) JOEP and (c) JOSAN sampling locations. REY anomalies and ratios are calculated using the Aalenian calcareous sandstone-normalized patterns.

Figure 4: PAAS-normalized REY patterns of bedrocks covering the Orne River basin (a) and of the three selected riverbank cores normalized by the SiO_2 content (b: BETHUP, c: JOEP, d: JOSAN). The groups are defined according to Kanbar et al. (2017).

3.3. REY patterns, concentrations and major element concentrations in the leachates and residual fractions

The REY concentrations in the leachates of the first two steps of the sequential extraction (water and 0.05N Hac) were negligible and most often below the detection limits. Therefore, only the results related to the two last leaching steps, using 1N HCl (L3) and 2N HNO_3 (L4), and the residual (R) fractions are reported. The samples from the surface and the deepest layers have very contrasting results.

At the surface, in JOSAN sample, the leaching yield ranged between 20% for Lu and 41% for Eu and Gd (Fig. 5a). This indicates that the middle REY were the most leached during the entire extraction procedure. REY were more concentrated in HCl compared to HNO_3 leachates. The PAAS-normalized REY patterns related to these last two extraction steps have differences in their Eu/Eu^*, La_N/Lu_N and Y/Ho ratios. HCl leachates present higher La_N/Lu_N (1.5 *vs.* 1.1) and Y/Ho (33 *vs.* 23) ratios than HNO_3, whereas HNO_3 leachates have higher Eu/Eu^* (1.3 *vs.* 1.1) (Fig. 5a). As a result, the pattern of the residual fraction is flat, illustrating that most of the mineral fractions that contributed to this middle REY enrichment were leached during the sequential extraction process and that, according to PAAS, the residue presents lower REY concentrations but similar REY distribution.

In the JOEP sample, the leaching yield ranged from 78% for Lu and more than 90% for Eu and the heavy REY were the less leached (Fig.5b). In comparison to the previous sample at JOSAN, the PAAS-normalized patterns of the two leachates are similar with HCl leachate being about two times more concentrated. They look like very similar to the pattern of the bulk sediment sample described previously (Fig. 4bc). As a consequence, the PAAS-normalized pattern of the residual fraction is strongly depleted in light and medium REY and present the lowest La_N/Lu_N ratio measured for all samples (0.2).

Figure 5: Contribution of leachates L3 and L4 (blue vertical bars) and residual R (grey vertical bars) fractions and related PAAS-normalized REY patterns (lines) in (a) the Group I (at JOSAN) and (b)

Group IV (at JOEP). White circles correspond to the bulk sample before leaching whereas the green, the orange and the dark grey represent the 1N HCl (L3), 2N HNO_3 (L4) and residual (R) fractions, respectively.

The sequential extractions performed for the major elements on the two selected samples corroborate most of the REY results. In the JOSAN sample, Na, Mg, K, Al and Fe are mainly contained in the residual fraction and present extraction yields below 20% (Fig. 6a), whereas Ca (98%), Mn (63%) and P (32%) are more labile and mainly present after L2 and L3 for Ca and after L3 and L4 for Mn and P. The partitioning of Ca, Mn and P between the different leachates of JOEP sample and the respective extraction yields are very similar to JOSAN (Fig. 6b). However, P is distributed among less labile fractions in JOEP and mainly present in L4 leachates. All the other elements, except K, present larger extraction yields in comparison to JOSAN, from 28% for Fe to 74% for Na.

Figure 6: Extraction yield and contribution of leachates (blue vertical bars) and residual (grey bars) fractions of total REY and related major element concentrations in the Group I at JOSAN (a) and Group IV at JOEP (b). Leachate with MilliQ water (L1); leachate with 0.05N Hac (L2), leachate with 1N HCl (L3); leachate with 2N HNO_3 (L4); residual fraction (R).

4. Discussion

4.1. Lithological heritage on the REY pattern of the core surface layer (Group I)

The REY normalized patterns of the surface sediments present strong similarities with the Toarcian marls that cover about 70% of the basin area (Fig. 1). Both bedrock and surface sediment samples have, according to PAAS, La_N/Lu_N ratios about 1 and slight upward convexities for the middle REY (MREY) explained by Eu/Eu^* about 1.2 (Fig. 3 and 4). One of the main differences is the Y content that is depleted in the surface sediments, with a Y/Ho ratio about 27, when Y/Ho ratio is 32 in the lithology. The MREY enrichments are also like those of suspended sediments transported larger world rivers as the Congo, Amazon, Mississippi, Ohio, and Rhine Rivers (Goldstein and Jacobsen, 1988; Elderfield et al., 1990; Dupré et al., 1996; Tricca et al., 1999; Klaver et al., 2014). This enrichment might be related to the presence of phosphate minerals because many phosphatic minerals of not only biogenic, authigenic and diagenetic origins, but also magmatic origins show this upward convexity (Hannigan and Sholkovitz, 2001; Stille et al., 2009). As already shown by Hissler et al. (2016) and more recently by Martin et al. (2021) in the neighbouring Alzette River basin in Luxembourg, the soils surrounding this latter area display P- and REY-bearing mineral phases that can characterize similar weak MREY enrichments. The geology that constitutes the Orne River and the upper Alzette River are the same and we expect similar mineral contribution and related REY pattern of the suspended particles originated from the soil erosion in the Orne watershed.

This assumption is also strengthened by the results obtained with the sequential extraction performed on the JOSAN sample. The mineral fractions related to the MREY enrichment were completely leached after the entire extraction procedure (Fig. 5a). MREY extraction yield were the highest, between 38 and 41% of the total REY content. As a result, the MREY enrichment disappeared in the PAAS-normalized pattern of the residual fraction no with $Eu/Eu^* = 1.1$. The L3 and L4 leachates do not show similar PAAS-normalized REY distribution patterns. Most enriched in REY is L3 with a MREY and Y enrichments and a HREY depletion. L4 is characterized by MREY enrichment and LREY, HREY

and Y depletions. Based on these results, we can state that L3 and L4 leachates represent two distinct phases of minerals that are progressively leached from pH=3.0 (L3) to pH<1.0 (L4); these conditions could dissolve MREY-bearing phosphate, like apatite, monazite, xenotime or rhabdophane minerals (Hissler et al., 2015b). Indeed, the LREY depletion accompanied with the MREY enrichment in L4 is typical to the apatite REY pattern, as observed by Aubert et al. (2001). Additionally, most of the phosphorous (22%) was leached during L4 extraction step (Fig. 6a). Therefore, the REY composition of the surface sediment collected at the three locations originate from the erosion of the surrounding and upstream soils. They have been progressively transported from their source, in the upstream agricultural part of the basin, to the Orne River during successive flood events. Our results may also show that during fluvial transport of the soil particles, Y could be preferentially leached in comparison to Ho, as seen in Fig. 4.

4.2. Origin of the REY pattern found in deep core layers.

Very different is the PAAS-normalized REY pattern of the steel production wastes that constitute the deeper layers of the JOEP and BETHUP cores. As shown in Fig. 3 and 4, their REY distribution is unusual in comparison to lithological pattern from Group I found for the surface layers of the three cores. Two main characteristics can define the different pattern of Group IV samples.

The first characteristic is the important depletion of LREY compared to MREY and HREY and coupled with a Y depletion. These depletions are represented by La_N/Lu_N, La_N/Gd_N ratios ranging from 0.40 to 0.50 and a Y/Ho ratio about 25 (Fig. 4). These characteristics are very close to the ratios that characterize the Aalenian calcareous sandstone (Fig. 7), which was used as iron ore for the local steel production in the Orne River valley (Kanbar et al., 2017). This latter presents La_N/Lu_N, La_N/Gd_N and Y/Ho ratios of 0.40, 0.40 and 24, respectively. We assume here that these two characteristic depletions originate from the initial REY signature of the iron ore and that these REY characteristics were preserved during the melting process inside the blast furnaces or converters of steel-making facilities.

Figure 7: Aalenian calcareous sandstone-normalized REY patterns for the 16 riverbank samples of group IV at JOEP and BETHUP. The black line corresponds to the average value and the light grey area to the standard deviation (n=16).

The second characteristic is the enrichments in Ce, Sm, Eu, Tm and Yb in comparison to the surface layers (Fig. 4). All these enrichments present good level of correlations and by comparing them using single linear regression (Fig. 8), different regression slopes allow to group these five anomalies according to the 1:1 line. This statistical analysis suggests that especially Eu and Yb anomalies, but also Sm anomaly, behave more similarly than Ce and Tb anomalies. For this Group IV, we expected that the sequential extraction would reveal different chemical status for the REY anomalies. However, for JOEP samples, the amounts of chemically extracted REYs are closer to the total contents. The leaching yields range from 61 to 79% for the HREY, 80 to 87% for the MREY and 81 to 84% for the LREY (Fig. 5b). Interestingly, all REY anomalies previously identified in bulk samples are preserved in L3 and L4 leachates (Fig. 5b). Even the residual fractions have some remnant of the leached patterns. The used sequential leaching was not able to separate the different REY enrichments observed according to the supposed chemical status. For this group IV, the sequential extraction suggests that all observed REY enrichments may belong to same material phases formed during the melting/cooling processes of the pig iron and steel production.

Concerning the major elements, it appears that K, Al and Fe present the lowest leaching yields during the complete procedure (<50% of the total contents), and significantly lower than the yields for REY. These latter present closer results with Al, Mn and P (Fig. 6b), having respective leaching yield of 50, 73 and 54%. The similar leaching yields of Al, Mn, P and REY (L3 and L4) support that REY leached from JOEP are linked to Al, Mn and P phases that formed in the blast furnace during steel production. However, as the mineralogy analysis demonstrated the presence of numerous iron oxides, we might also take into account that only a fraction of iron bearing phases was efficiently leached).

The fractionation of the different lanthanides was certainly controlled by processes that can target lanthanides having very distinct physical properties and distributed over the entire REY spectra from LREY to HREY. Temperature (up to 1200-1300 °C) and oxygen conditions within the blast furnaces have certainly induced this partitioning. As experimented by Ingrao et al. (2019), the positive Eu/Eu^*, Yb/Yb^* and Sm/Sm^* anomalies observed in this study can be attributed to the preferential incorporation of these elements in their divalent state in the furnace fumes. Reducive conditions can be at the origin of these anomalies by enhancing the formation of divalent species Eu^{2+}, Yb^{2+} and Sm^{2+}. Previous studies also suggested that in such conditions, only one phase seems controlling the REY budget and that Eu and Yb anomalies are attributed to preferential evaporation and condensation of the REY (Lodders, 1996; Dickinson and McCoy 1997).

However, Ce and Tm enrichments might have different explanations. Indeed, Ce naturally occurs in two different valence states according to redox conditions Ce^{III} to Ce^{IV}. The positive anomaly of Ce can only form during specific oxidative conditions, as this oxidation to Ce^{IV} is combined with the formation of CeO_2 and enhances the adsorption of Ce on mineral phases (Braun et al., 1990). The process leading to the Ce anomaly could be related to the latest stage of the waste material production when oxidative conditions took place during the cooling or wet cleaning of fumes. Supplementary analyses are necessary, such as the investigation of Ce^{IV}/Ce^{III} ratio.

Figure 8: Relationship between Eu/Eu* and related REY anomalies calculated for the core riverbank samples at BETHUP location. The color refers to the group of REY defined in Fig. 4.

4.3. Natural sediment *vs.* steel industry waste: a two end-member mixing in the riverbank system

Figures 3 and 4 show how the different REY pattern characteristics progressively evolve in between two end-members: (i) the surface layer of the riverbank cores, also identified as Group I at BETHUP sampling site, and (ii) the bottom layers corresponding to the industrial waste released in the river and referred to as Group IV. La_N/Lu_N and Y/Ho regularly decrease and the Eu, Yb, Sm, Ce and Tb enrichments regularly increase from Group I to Group IV. We also show that Group I and Group IV REY properties present very strong similarity with bedrocks, Toarcian marl and Aalenian calcareous sandstone, respectively. If we plot the different core samples and the two latter lithologies in a La_N/Lu_N *vs.* $\Sigma REY/SiO_2$ diagram, the riverbank layers at JOEP and BETHUP are distributed along a mixing curve between the Toarcian marls and the Aalenian sandstone (Fig.9).

For JOSAN core, we could not detect the presence of the industrial steel-making waste, the La_N/Lu_N remains stable about 0.8, and the core samples are out of the line between the two extremes Toarcian marl and Aalenian sandstone. Interestingly, the surface layers of the three cores present very similar La_N/Lu_N *vs.* $\Sigma REY/SiO_2$ values (Fig. 9).

This graph indicates that the intermediate layers of JOEP and BETHUP cores contain REY bearing phases from the soil erosion and from the steel-making activity. Detrital contribution was also

suggested in these deep core layers by the presence of quartz (XRD) and clay minerals (TEM analyses, Kanbar et al . 2017). From the beginning of steel production until the complete ending of the industrial activity, the industrial waste release was not constant, and due to environmental regulation in the 70s (Garcier al 2007) the volumes of industrial particles rejected to the river were significantly reduced. The distribution of REY in Group IV samples of JOEP and BETHUP cores may also highlight the different man induced activities performed in the vicinity of these two coring stations (quantity released in the riverbed, liming of industrial waste, different dredging events), as well as natural processes affecting the bank morphology (bioturbation, riverbank erosion/deposition during floods). Indeed, the material stored in BETHUP might display a sequence including the dredging period in the late 80's. JOEP banks display clear interlayers of lime sludge (fig. 2c) and is far more depleted in detrital minerals, with almost no Quartz detected from the XRD pattern (Fig. 2a). However, the little information that still exists on the history of this industrial valleys does not allow to reconstruct the precise chronology of the different sampling sites. However, the information gained in this study are of interest to quantify industrial waste contribution in the suspended sediment transported in the Orne River, especially after the opening of the dams that will generate higher erosion in the riverbed and increase the transport of REY polluted particles to the Orne River and downstream in the Moselle River.

Figure 9: Relationship between the sum of REY concentrations normalized by SiO_2 concentration and the PAAS-normalized La_N/Lu_N ratio for the riverbed sediment samples, the Toarcian marl and the Aalenian calcareous sandstone collected in the Orne River basin. Also are indicated on the mixing line the contribution, in %, of the industrial waste in the bulk core sediment samples. The color refers to the group of REY defined in Fig. 4.

5. Conclusion

Whereas the anthropogenic impact on colloidal and dissolved REY transported in rivers is now well established worldwide, there is still only few studies that detected any effect of human activity on suspended and riverbed sediments. This new contribution presents for the first time a direct and clear effect of an industrial process on the REY composition in riverbank sediments and on its temporal evolution after the decline of the industry.

The unusual REY patterns that were observed in the sediment of the Orne River are directly related to the past steel-making activity. The processes involved during the production of steel gave to the studied industrial waste a specific REY signature constituted by a heavy REY enrichment, originated from the used iron ore, and specific Ce, Sm, Eu, Tm and Yb enrichments. The fractionation that happened between these latter elements and the other lanthanides is certainly due to two processes. On the one hand, the reduction of the usual trivalent form to Eu^{2+}, Yb^{2+} and Sm^{2+} in the temperature and oxygen conditions inside the blast furnace. On the other hand, the oxidative conditions that took place during the waste material cooling may favour the precipitation and adsorption of Ce.

We also show that the REY trapped in the industrial waste, at the bottom of the riverbank sediments, is more labile than the REY transported on natural particles coming from soil erosion. They may present a higher potential to be mobilized from sediment particles to the water column. This is now a crucial issue in this river basin because of the opening of the dams that will increase the erosion of these contaminated sediments. However, the specific REY pattern that characterize them is a useful information to trace their fate and to evaluate potential biological and human health threats.

6. Supplementary material and data availability

The data used in this study are publicly available on ORDAR data repository for the total element content of all core samples (https://doi.org/10.24396/ORDAR-59) and on a Zenodo data repository for the sequential leaching analyses (https://doi.org/10.5281/zenodo.7447548).

7. References

Abuhelou, F., (2016). Spatial and temporal variations of the occurrence and distribution of polycyclic aromatic compounds in a river system affected by past industrial activities. PhD dissertation, Université de Lorraine, France.

Aubert, D., Stille, P., Probst, A. (2001). REE fractionation during granite alteration, soil formation, migration and removal by dissolved and suspended loads from small river systems in the Vosges mountains: chemical and Sr-Nd isotopic evidence. Geochim. Cosmochim. Acta 65 (3), 387–406. doi:10.1016/S0016-7037(00)00546-9

Bau, M., Dulski, P. (1996). Anthropogenic origin of positive gadolinium anomalies in river waters. Earth Planet. Sci. Lett. 143, 245−255. doi: 10.1016/0012-821X(96)00127-6

Braun, J.-J., Pagel, M., Muller, J.P., Bilong, P., Michard, A., Guillet, B. (1990). Cerium anomalies in lateritic profiles. Geochim. Cosmochim. Acta 54, 781–795. Doi: 10.1016/0016-7037(90)90373-S

Carignan, J., Hild, P., Mevelle, G., Morel, J., Yeghicheyan, D. (2001). Routine analyses of trace elements in geological samples using flow injection and low pressure on-line liquid chromatography coupled to ICP-MS: a study of geochemical reference materials BR, DR-N, UB-N, AN-G and GH. Geostand. Geoanal. Res. 25, 187–198. doi: 10.1111/j.1751-908X.2001.tb00595.x

Dagallier, G., Grgic, D., Homand, F. (2002). Caractérisation minéralogique et microtexturale du vieillissement anthropique du minerai de fer lorrain. CRGeosci. 334, 455–462. doi:10.1016/S1631-0713(02)01783-2

De la Cruz Barrón M, Merlin C, Guilloteau H, Montargès-Pelletier E and Bellanger X (2018). Suspended Materials in River Waters Differentially Enrich Class 1 Integron- and IncP-1 Plasmid-Carrying Bacteria in Sediments. Front. Microbiol. 9:1443. doi: 10.3389/fmicb.2018.01443

Dickinson, T. L., McCoy, T. (1997). Experimental rare-earth element partitioning in oldhamite: Implications for the igneous origin of aubritic oldhamite. Meteorit. Planet. Sci. 32, 395–412. doi: 10.1111/j.1945-5100.1997.tb01283.x

Dupré, B., Gaillardet, J., Rousseau, D., Allègre, C.J. (1996). Major and trace elements of riverborne material: the Congo Basin. Geochim. Cosmochim. Acta 60 (8), 1301–1321. doi: 10.1016/0016-7037(96)00043-9

Elderfield, H., Upstill-Goddard, R., Sholkovitz, E.R. (1990). The rare earth elements in rivers, estuaries, and coastal seas and their significance to the composition of ocean waters. Geochim. Cosmochim. Acta 54 (4), 971–991. Doi: 10.1016/0016-7037(90) 90432-K.

Garcier, R.J. (2007). Rivers we can't bring ourselves to clean – historical insights into the pollution of the Moselle River (France), 1850–2000. Hydrol. Earth Syst. Sci. 11: 1731–1745. doi: 10.5194/hess-11-1731-2007

Goldstein, S. J.; Jacobsen, S. B (1988). Nd and Sr isotopic systematics of river water suspended material: implications for crustal evolution. Earth Planet. Sci. Lett. 1988, 87, 249−265. doi: 10.1016/0012-821X(88)90013-1

Hannigan, R.E., Sholkovitz, E.R. (2001). The development of middle rare earth element enrichments in freshwaters: weathering of phosphate minerals. Chem. Geol. 175, 495-508. doi: 10.1016/S0009-2541(00)00355-7

Hissler, C., Stille, P., Iffly, J.F., Guignard, C., Chabaux, F., Pfister, L. (2016). Origin and Dynamics of Rare Earth Elements during flood events in contaminated river basins: Sr-Nd-Pb evidence. Environ. Sci. Technol. 50, 4624-4631. doi: 10.1021/acs.est.5b03660

Hissler, C., Hostache, R., Iffly, J.F., Pfister, L., Stille, P. (2015a) Anthropogenic rare earth element fluxes into floodplains: coupling between geochemical monitoring and hydrodynamic-sediment transport modelling. CRGeosci. 347, 294–303. doi: 10.1016/j.crte.2015.01.003

Hissler, C., Stille, P., Juilleret, J., Iffly, J.F., Perrone, T., Morvan, G. (2015b). Elucidating the formation of terra fuscas using Sr-Nd-Pb isotopes and rare earth elements. Appl. Geochem. 54, 85-99. doi: 10.1016/j.apgeochem.2015.01.011

Ingrao, N.J., Hammouda, T., Boyet, M., Gaborieau M., Moine B.N., Vlastelic, I., Bouhifd, M.A., Devida J.-L., Mathon, O., Testemale D. (2019). Rare earth element partitioning between sulphides and melt: Evidence for Yb2+ and Sm2+ in EH chondrites. Geochim. Cosmochim. Acta 265, 182–197. doi: 10.1016/j.gca.2019.08.036

Kanbar, H.J., Montargès-Pelletier, E., Losson, B., Bihannic, I., Gley, R., Bauer, A., Villieras, F., Manceau, L., El Samrani, A.G., Kazpard, V., Mansuy-Huault, L. (2017). Iron mineralogy as a fingerprint of former steelmaking activities in river sediments. Sci. Tot. Environ. 599-600, 540-553. doi: 10.1016/j.scitotenv.2017.04.156

Kanbar, H. J. (2017). What the Orne River tells about the former steelmaking activities: chemical and mineralogical investigations on sediments. PhD dissertation, Université de Lorraine, France.

Klaver, G., Verheul, M., Bakker, I., Petelet-Giraud, E., Négrel, P. (2014). Anthropogenic rare earth element in rivers: gadolinium and lanthanum. Partitioning between the dissolved and particulate phases in the Rhine River and spatial propagation through the Rhine-Meuse Delta (the Netherlands). Appl. Geochem. 47, 186–197. doi: 10.1016/j.apgeochem.2014.05.020

Knobloch, V., Zimmermann, T., Gößling-Reisemann, S., (2018). From criticality to vulnerability of resource supply: the case of the automobile industry. Resour. Conserv. Recycl. 138, 272–282. doi: 10.1016/j.resconrec.2018.05.027

Kulaksiz, S., Bau, M. (2013). Anthropogenic dissolved and colloid/nanoparticle-bound samarium, lanthanum and gadolinium in the Rhine River and the impending destruction of the natural rare earth element distribution in rivers. Earth Planet. Sci. Lett. 362, 43–50. doi: 10.1016/j.epsl.2012.11.033

552 Lachaux, N., Cossu-Leguille, C., Poirier, L., Gross, E.M., Giamberini L (2022)., Integrated
553 environmental risk assessment of rare earth elements mixture on aquatic ecosystems. Front. Environ.
554 Sci. 10:974191. doi: 10.3389/fenvs.2022.974191

555 Lodders, K. (1996). An experimental and theoretical study of rare earth element partitioning between
556 sulfides (FeS, CaS) and silicate and applications to enstatite achondrites. Meteorit. Planet. Sci. 31, 749–
557 766. doi: 10.1111/j.1945-5100.1996.tb02110.x

558 Losson, B., Manceau, L., Kanbar, H.J., Waldvogel, Y., Delus, C., Mansuy- Huault, L., Hissler, C.,
559 Montargès-Pelletier, E. (2020). Hydrodynamique de l'Orne et mobilisation sédimentaire dans la zone
560 de remous amont du barrage de Beth (Lorraine, France). Géomorphologie : relief, processus,
561 environnement. doi: 10.4000/geomorphologie.14004

562 Louis, P., Messaoudene, A., Jrad, H., Abdoul-Hamid, B.A., Vignati, D.A.L., Pons, M.-N. (2020).
563 Understanding rare earth elements concentrations, anomalies and fluxes at the river basin scale: the
564 Moselle River (France) as a case study. Sci. Total Environ. 742, 140619. doi:
565 10.1016/j.scitotenv.2020.140619

566 Martin, L.A., Vignati, D.A.L., Hissler, C. (2021). Contrasting distribution of REE and yttrium among
567 particulate, colloidal and dissolved fractions during low and high flows in peri-urban and agricultural
568 river systems. Science of Total Environment 790: 148207. doi: 10.1016/j.scitotenv.2021.148207

569 Martínez-Carreras, N., Ogorzaly, L., Walczak, C., Merlin, C., Montargès-Pelletier, E., Gantzer, C.,
570 Iffly, J.F., Cauchie, H.-M., Hissler, C. (2021). F-Specific RNA Bacteriophage Transport in
571 StreamWater: Hydro-Meteorological Controls and Association with Suspended Solids. Water 2021,
572 13, 2250. doi: 10.3390/w13162250

573 Merschel, G., Bau, M., Baldewein, L., Dantas, E.L., Walde, D., Bühn, B. (2015). Tracing and tracking
574 wastewater-derived substances in freshwater lakes and reservoirs: anthropogenic gadolinium and
575 geogenic REEs in Lake Paranoá, Brasilia. CRGeosci. 347, 284–293. doi: 10.1016/j.crte.2015.01.004

576 Parant, M., Perrat, E., Wagner, P., Rosin, C., Py, J.-S., Cossu-Leguille, C. (2018). Variations of
577 anthropogenic gadolinium in rivers close to waste water treatment plant discharges. Environ. Sci.
578 Pollut. Res. 25, 36207–36222. doi : 10.1007/s11356-018-3489-6

579 Picon, M. (2014). Autour de l'Orne industrieuse: paysages industriels hérités. Environmental
580 Engineering; Université de Lorraine. <dumas-01110255>

581 Steinmann, M., Stille, P. (1997). Rare earth element behavior and Pb, Sr, Nd isotope systematics in a
582 heavy metal contaminated soil. Appl. Geochem. 12, 607–624. doi: 10.1016/S0883-2927(97)00017-6

583 Stille, P., Pierret, M.-C., Steinmann, M., Chabaux, F., Boutin, R., Aubert, D., Pourcelot, L., Morvan,
584 G. (2009). Impact of atmospheric deposition, biogeochemical cycling and water-mineral interaction on
585 REE fractionation in acidic surface soils and soil water (the Strengbach case). Chem. Geol. 264, 173–
586 186. doi: 10.1016/j.chemgeo.2009.03.005

587 Stille, P., Clauer, N. (1994). The process of glauconitization: chemical and isotopic evidence. Contrib.
588 Mineral. Petrol. 117, 253–262. doi: 10.1007/BF00310867

589 Taylor, S.R., McLennan, S.M., (1985). The Continental Crust: Its Composition and Evolution.
590 Blackwell, Oxford, 312p.

591 Tricca, A., Stille, P., Steinmann, M., Kiefel, B., Samuel, J., Eikenberg, J. (1999) Rare earth elements
592 and Sr and Nd isotopic compositions of dissolved and suspended loads from small river systems in the
593 Vosges mountains (France), the river Rhine and groundwater. Chem. Geol. 160, 139−158. doi:
594 10.1016/S0009-2541(99)00065-0

595 Vdović, N., Billon, G., Gabelle, C., Potdevin, J.-L., 2006. Remobilization of metals from slag and
596 polluted sediments (case study: the canal of the Deûle River, northern France). Environ. Pollut.
597 141:359–369. doi: 10.1016/j.envplo.2005.08.034

598 Zebracki, M. (2008). Devenir des polluants métalliques associés aux sédiments contaminés dans un
599 cours d'eau en relation avec la dynamique sédimentaire. PhD dissertation, Université Paris-Sud XI,
600 France.

601 Zhang, S., Ding, Y., Liu, B., Chang, C. (2017). Supply and demand of some critical metals and present
602 status of their recycling in WEEE. Waste Manag. 65, 113–127. doi: 10.1016/j.wasman.2017.04.003.

Figure 1.JPEG

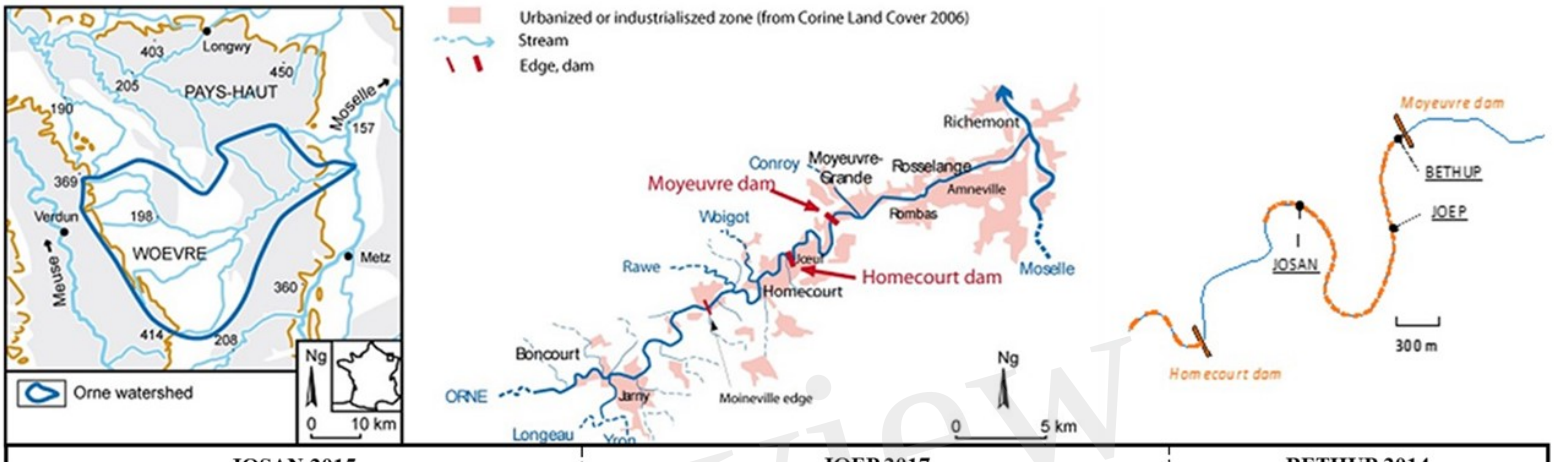

JOSAN 2015

4 — 0 Brown sediments, wet and poorly cohesive
Fine brown sediments, leaves, roots
16.5 Black sediment, bedded by thick layers of whole leaves.
27.5
30 — Grey sand with shell parts
32 Black sediment, bedded by thick layers of whole leaves.
44
47.5 — Coarse sand with shell parts
51.5 cm

JOEP 2017

0 Brown and fine sediment, roots
12 Brown and fine sediment, clayey like, fine roots
18 Light brown sediment, rust dots
25 Black and fine grained layer, wood pieces, shiny black particles
40 Muddy black-grey layer, shiny black particles
49 Muddy black layer, clayey like, plant residues
57 Black indured layer, few submillimetric layers with shiny and white particles
82 cm

BETHUP 2014

0 Brown and fine sediments, wet and poorly cohesive
10 Shining black clayey like
38 Sandy layer
42 Black grey fine grained
50 Black, fine grained, clayey like, oil smell
131 cm

Figure 2.JPEG

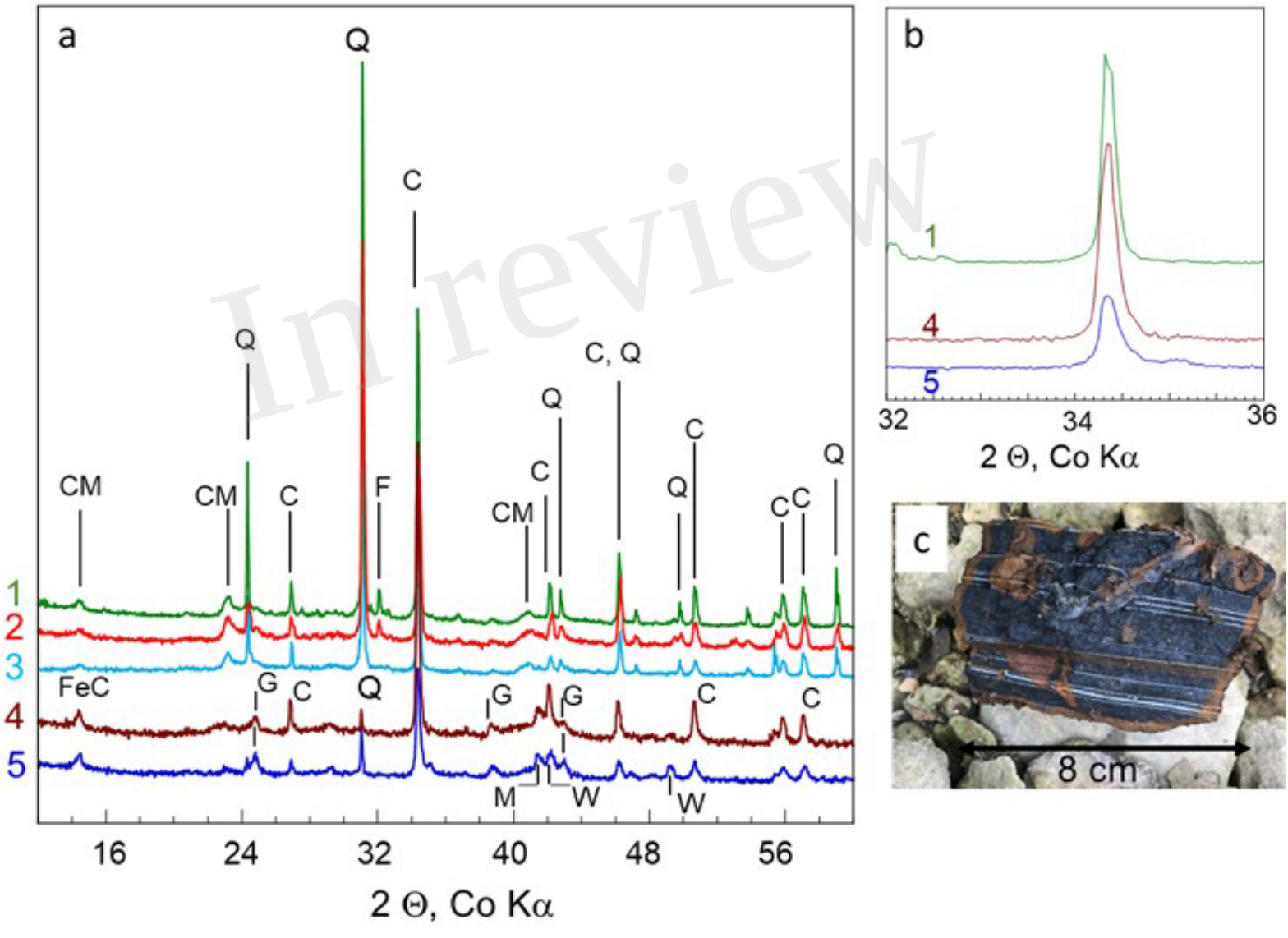

Figure 3.JPEG

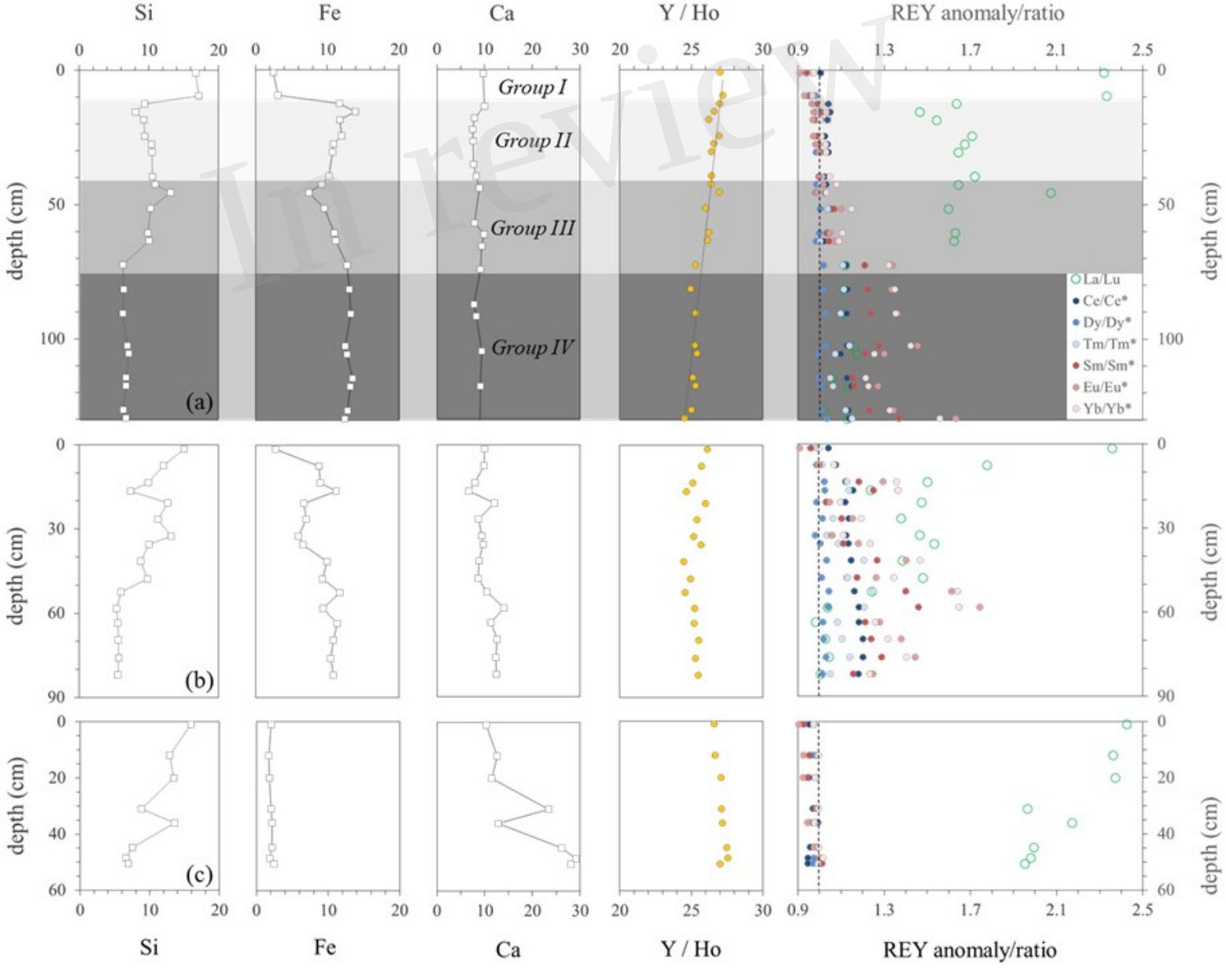

Figure 4.JPEG

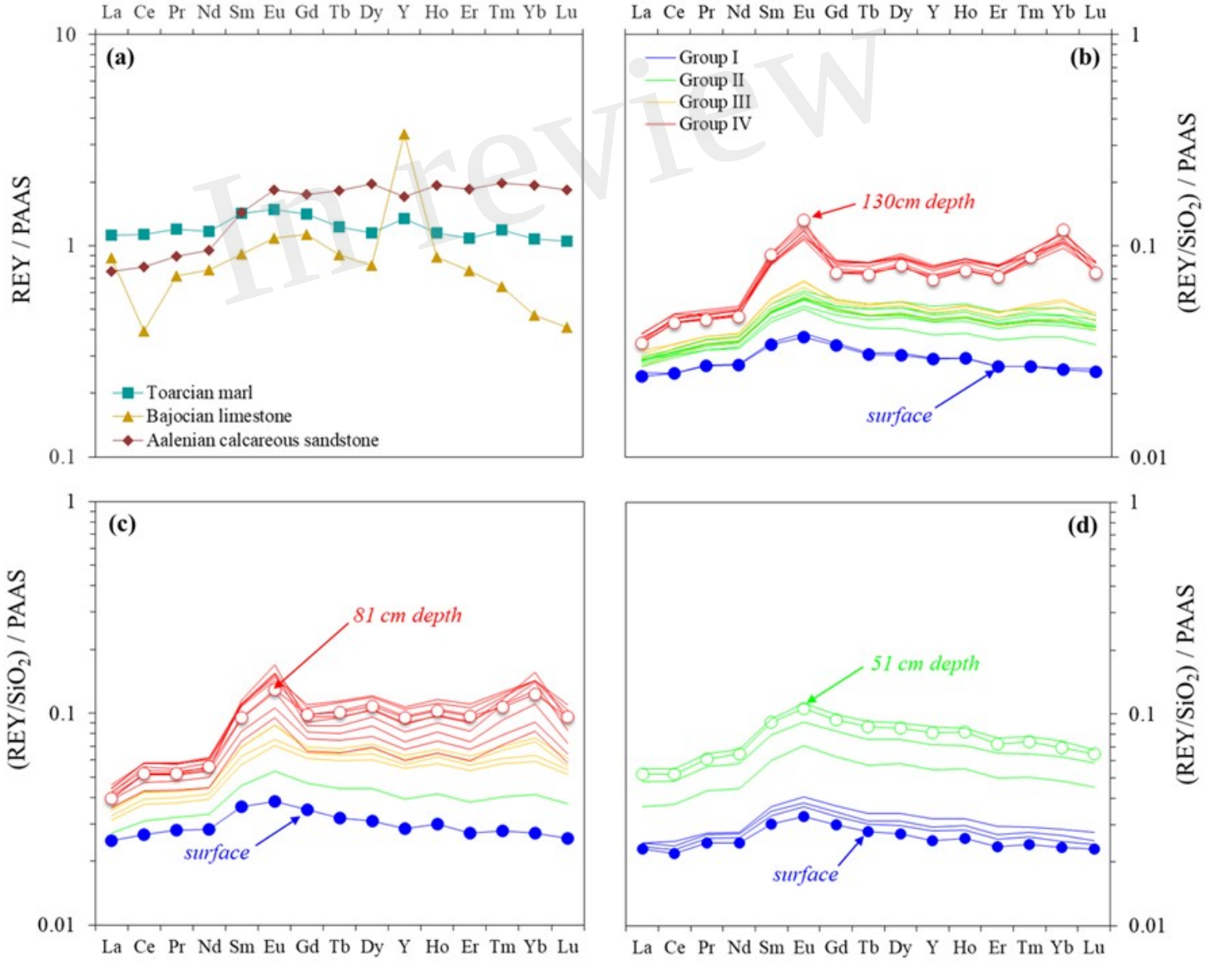

Figure 5.JPEG

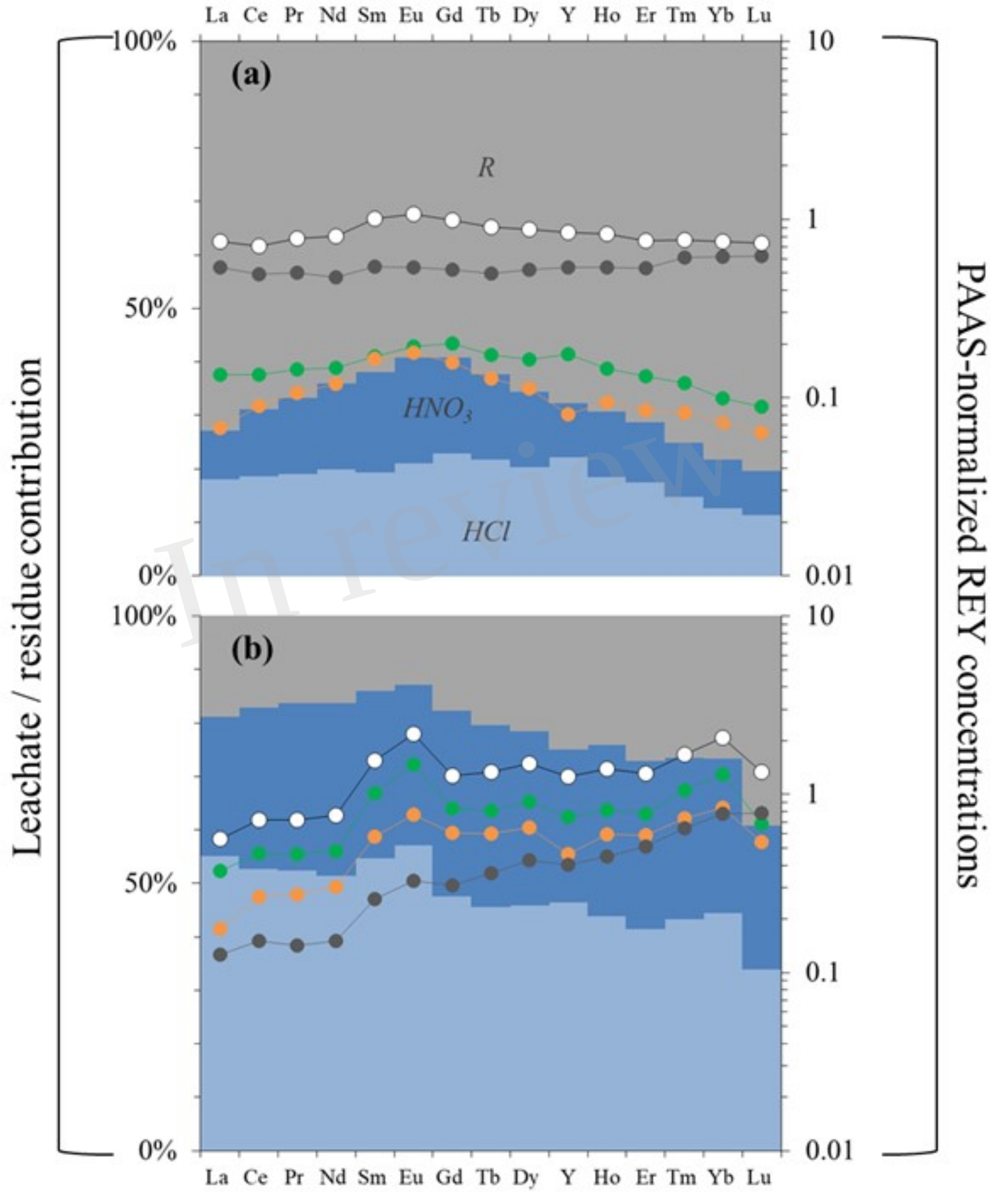

Figure 6.JPEG

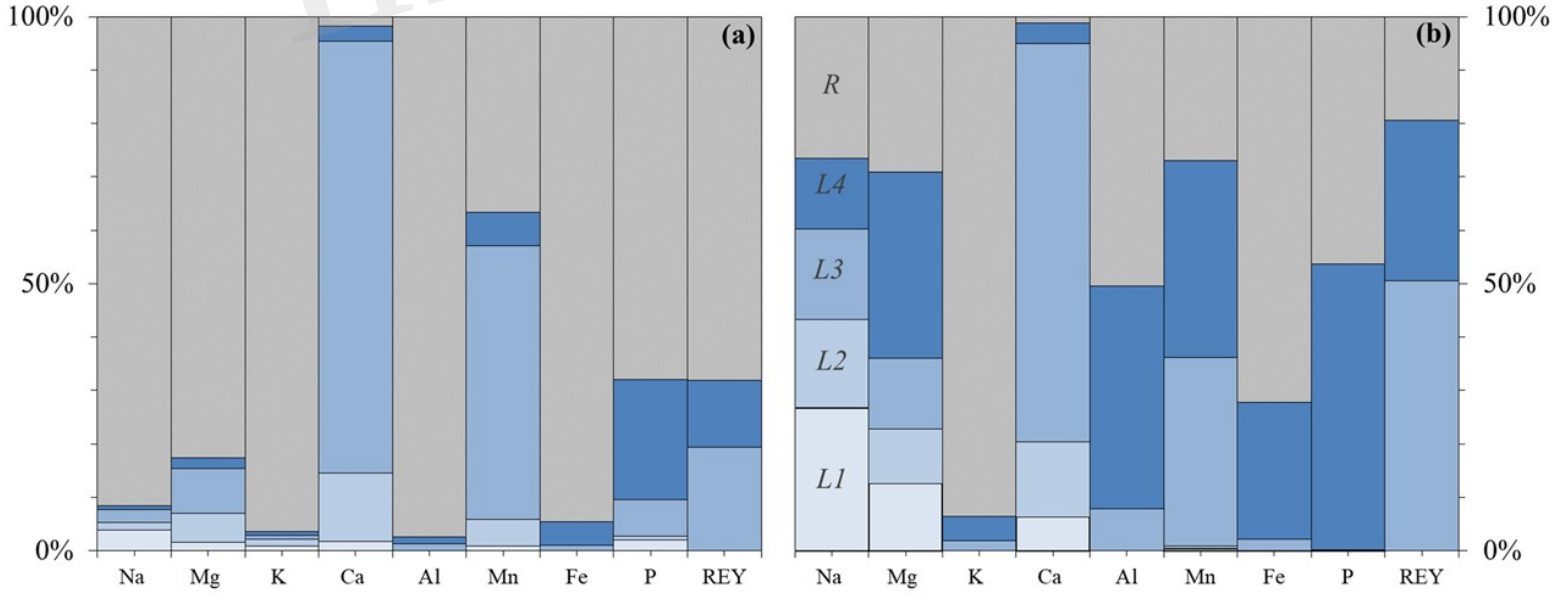

Figure 7.JPEG

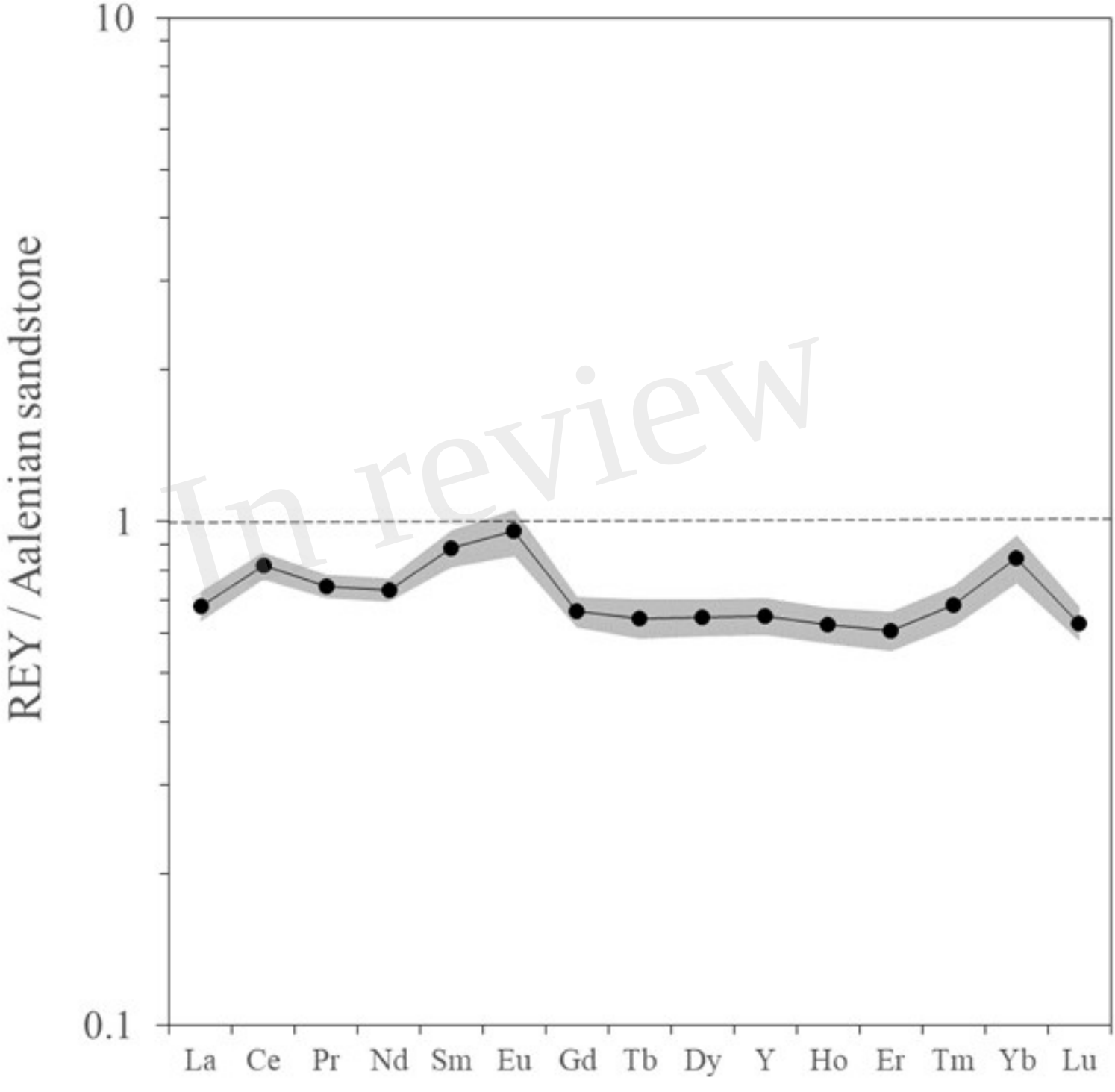

Figure 8.JPEG

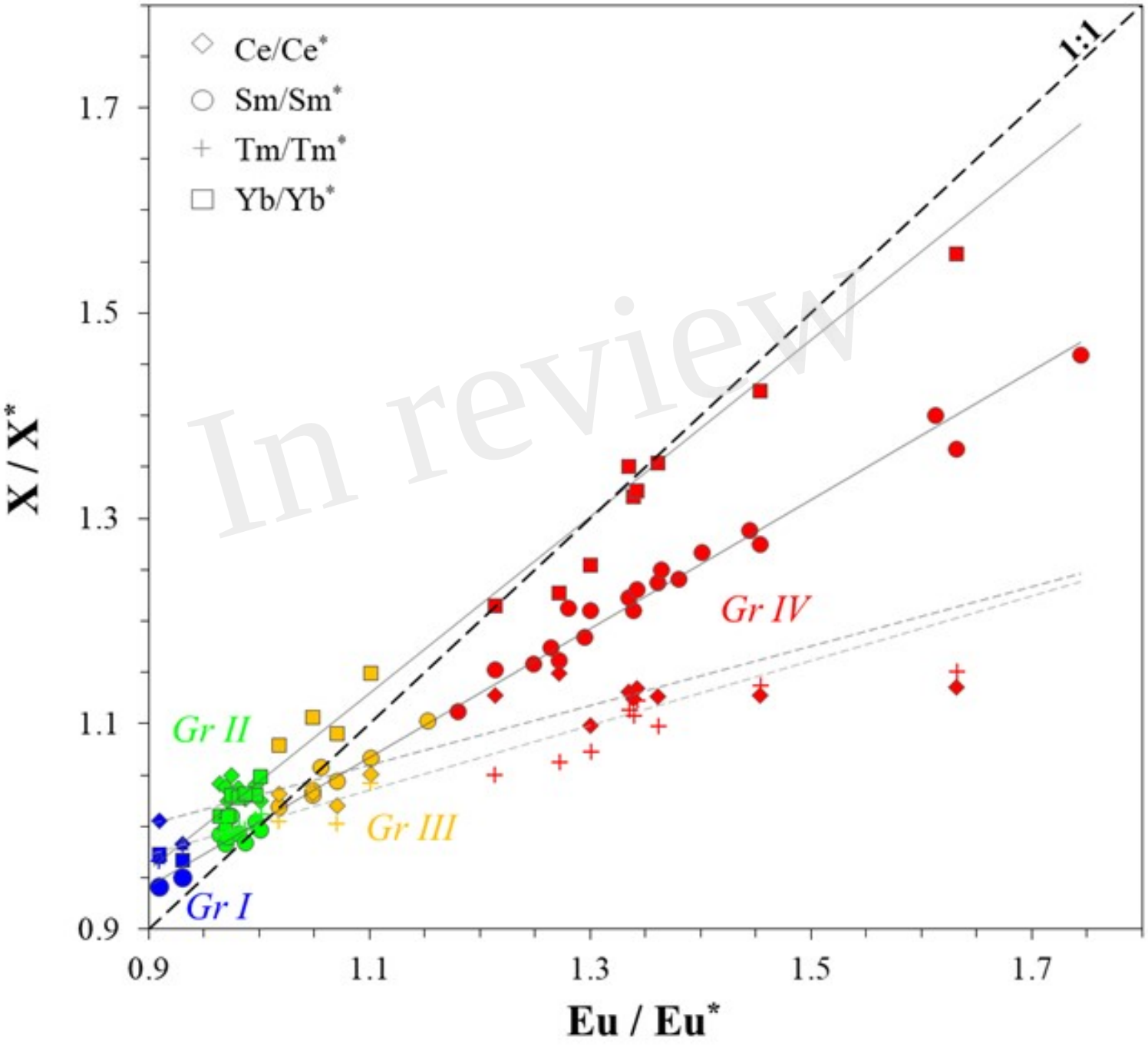

Figure 9.JPEG